SYNTHETIC BIOLOGY

Programming self-organizing multicellular structures with synthetic cell-cell signaling

Satoshi Toda[1], Lucas R. Blauch[2], Sindy K. Y. Tang[2], Leonardo Morsut[1]*†, Wendell A. Lim[1]†

A common theme in the self-organization of multicellular tissues is the use of cell-cell signaling networks to induce morphological changes. We used the modular synNotch juxtacrine signaling platform to engineer artificial genetic programs in which specific cell-cell contacts induced changes in cadherin cell adhesion. Despite their simplicity, these minimal intercellular programs were sufficient to yield assemblies with hallmarks of natural developmental systems: robust self-organization into multidomain structures, well-choreographed sequential assembly, cell type divergence, symmetry breaking, and the capacity for regeneration upon injury. The ability of these networks to drive complex structure formation illustrates the power of interlinking cell signaling with cell sorting: Signal-induced spatial reorganization alters the local signals received by each cell, resulting in iterative cycles of cell fate branching. These results provide insights into the evolution of multicellularity and demonstrate the potential to engineer customized self-organizing tissues or materials.

During the development of multicellular organisms, tissues self-organize into the complex architectures essential for proper function. Even with minimal external instructions, cells proliferate, diverge into distinct cell types, and spatially self-organize into complex structures and patterns. Such self-organized structures are radically different from most human-made structures, because they are not assembled from preexisting parts that are physically linked according to a defined Cartesian blueprint. Rather, these structures emerge through a series of genetically programmed sequential events. To test and better develop our understanding of the principles governing multicellular self-organization, it would be powerful to design synthetic genetic programs that could direct the formation of custom multicellular structures (*1*–*7*).

Extensive studies of natural developmental programs have implicated many genes that control cell-cell signaling and cell morphology. Despite their molecular diversity, a common theme in these developmental systems is the use of cell-cell signaling interactions to conditionally induce morphological responses (*8*, *9*). Thus, we explored whether simple synthetic circuits in which morphological changes are driven by cell-cell signaling interactions could suffice to generate self-organizing multicellular structures.

A simple toolkit for engineering morphological programs

As a modular platform for engineering new, orthogonal cell-cell signaling networks, we focused on using the synthetic notch (synNotch) receptor system (Fig. 1A). SynNotch receptors contain the core regulatory domain of the juxtacrine signaling receptor Notch, linked to a chimeric extracellular recognition domain (e.g., single-chain antibody) and a chimeric intracellular transcriptional domain (*10*). When it recognizes its cognate ligand on a neighboring cell, the synNotch receptor undergoes cleavage of the transmembrane region, releasing the intracellular transcriptional domain to enter the nucleus and drive the expression of user-specified target genes. Thus, we can design synthetic cell-cell communication programs using synNotch circuits. SynNotch receptor-ligand pairs do not cross-talk with native signaling pathways such as Notch-Delta, or with one another, as long as they have different recognition and transcriptional domains. Here, we used two synNotch receptor-ligand pairs—an anti-CD19 single-chain antibody (scFv) receptor paired with CD19 ligand, and an anti–green fluorescent protein (GFP) nanobody receptor paired with surface GFP ligand—as orthogonal cell-cell communication channels.

We created potential developmental programs by linking synNotch signaling to two possible transcriptional outputs: (i) expression of specific cadherin molecules (E-, N-, and P-cadherins), which lead to homotypic cell-cell adhesion and differential sorting of cells expressing different classes of adhesion molecules (*11*–*13*); and (ii) expression of new synNotch ligands (Fig. 1A). Morphological sorting driven by cadherin expression can change what cells are next to each other, thus altering what synNotch signals will or will not be transmitted. Similarly, expression of new synNotch ligands can also create a subsequent stage of new cell-cell signals. Consequently, both of these outputs can propagate regulatory cascades by generating new signaling interactions between cells in the collective assembly.

We also constructed the synNotch circuits so that they drive expression of different fluorescent proteins, allowing color to indicate "differentiation" into new cell types (Fig. 1B). We expressed these synNotch circuits in mouse L929 fibroblasts, placed the cells in a low-adhesion U-bottom well (*14*), and followed their organization over time by fluorescence microscopy. L929 cells do not self-organize; normally, they only form a loose and randomly organized multicellular aggregate. We then tested whether any of the synthetic circuits we constructed from this small set of components could drive higher-order self-organization.

Engineering interacting cells that self-organize into a two-layer structure

We first focused on engineering two cell types that, when mixed, might communicate with and activate one another to induce the formation of a self-organized structure. We engineered a sender cell that expresses the synNotch ligand CD19 and blue fluorescent protein (BFP) (cell A) and a receiver cell that expresses the cognate anti-CD19 synNotch receptor and its response element (cell B). To induce cell sorting as an output of synNotch signaling, we placed the E-cadherin (Ecad) and GFP genes under the control of the synNotch-responsive promoter in the receiver cells (cell B in Fig. 2A). The circuit is represented by the following scheme:

[**cell A:** CD19] → [**cell B:** αCD19 synNotch → $Ecad^{hi}$ + GFP]

As predicted, when cocultured with A-type sender cells, B-type receiver cells were activated to express Ecad and GFP (C-type cell phenotype). Subsequently, the green (GFP) C-type cells self-sorted to form a tight inner core, resulting in a well-defined two-layer structure (Fig. 2, B and C). Without induction of Ecad, the A- and B-type cells remained well-mixed (fig. S1A). When the synNotch signaling was inhibited by the γ-secretase inhibitor (2*S*)-*N*-[(3,5-difluorophenyl)acetyl]-L-alanyl-2-phenylglycine 1,1-dimethylethyl ester (DAPT), which blocks synNotch cleavage and signaling, sorting into two layers did not occur, as the inhibitor blocked the Ecad induction response in B-type cells (fig. S1B).

Using a bidirectional signaling cascade to engineer a self-organizing three-layer structure

To create more a complex structure, we added an additional layer of reciprocal cell-cell signaling to the above two-layer circuit (Fig. 2D). We engineered

[1]Department of Cellular and Molecular Pharmacology, Howard Hughes Medical Institute, and Center for Systems and Synthetic Biology, University of California, San Francisco, CA 94158, USA. [2]Department of Mechanical Engineering, Stanford University, Stanford, CA 94305, USA.
*Present address: Eli and Edythe Broad CIRM Center for Regenerative Medicine and Stem Cell Research, University of Southern California, Los Angeles, CA 90033, USA.
†Corresponding author. Email: leonardo.morsut@med.usc.edu (L.M.); wendell.lim@ucsf.edu (W.A.L.)

the receiver (B-type) cell so that in addition to inducibly expressing Ecad, it also inducibly produced surface-tethered GFP as a synNotch ligand (GFP_{lig}). This modified form of GFP is constructed by fusion with the platelet-derived growth factor receptor transmembrane (PDGFR TM) domain (*10*). Surface-tethered GFP served as both a fluorescent reporter of the new cell type and a ligand for a secondary synNotch receptor with the cognate anti-GFP nanobody binding domain. In the sender cells, which constitutively express BFP and CD19 ligand, we also expressed the anti-GFP synNotch receptor, which when induced would drive expression of a low amount of E-cadherin ($Ecad^{lo}$) fused with an mCherry reporter for visualization. Thus, the interaction between this pair of cell types can in principle yield a two-step cascade of reciprocal signaling: In the first step, CD19 on cell A activates anti-CD19 synNotch in cell B to induce expression of a high level of E-cadherin ($Ecad^{hi}$) and the GFP_{lig}. In the second step, the GFP_{lig} on cell B can reciprocally activate the anti-GFP synNotch receptors in neighboring A-type cells to induce a low level of E-cadherin alongside the mCherry reporter. In this case, the A-type cell starts out as a sender cell but later becomes a receiver cell. The circuit is represented by the following scheme:

[**cell A:** CD19; αGFP synNotch]
→ [**cell B:** αCD19 synNotch → $Ecad^{hi}$ + GFP_{lig}]
→ [**cell A:** αGFP synNotch → $Ecad^{lo}$ + mCherry]

This circuit was predicted to form a three-layer structure: a green internal core ($Ecad^{hi}$ + GFP) with the highest homotypic adhesion, an outer layer of blue cells (no Ecad), and a new population of red ($Ecad^{lo}$ + mCherry) cells at a middle interface layer (Fig. 2E). We first engineered and established cell A and cell B lines from single-cell clones, and then confirmed that they showed synNotch-driven expression of high or low amounts of Ecad along with the appropriate marker fluorescent proteins (fig. S2A).

When we cocultured 200 A-type cells and 40 B-type cells, a three-layer structure was robustly formed, with a development process that required ~20 hours to fully unfold (Fig. 2F, fig. S2B, and movie S1). The structure emerged in a stereotypical stepwise fashion: induction of the green cells, sorting to form an inner core, and then the formation of a red middle layer. Here, the cascade of cell sorting and reciprocal signaling from the green core cells drives fate branching of the original A-type sender cells into two distinct fates (red and blue). Thus, this program has substantial ordering power: (i) The program generates an increased number of cell types (two cell genotypes become three phenotypic cell types), and (ii) the program leads to spatial sorting into three distinct compartments. This change represents a decrease in entropy relative to the starting point of a random mixture of two cell types, as shown in the cell lineage map (Fig. 2E). Many of these features of increased self-ordering observed in this engineered assembly mimic the behavior of natural developmental systems, such as the simple formation of distinct progenitor cell types in early embryogenesis (*15*, *16*).

The observed self-organization could be blocked by disrupting either synNotch signaling or cadherin expression. When we blocked cell-cell signaling with an inhibitor of synNotch signaling (DAPT), we observed no increase in cell types and no cell sorting into distinct layers (Fig. 2G and fig. S3B). When we removed E-cadherin expression from the system (fig. S3A), the assembled cells induced expression of the GFP and mCherry markers, but the different cell types remained randomly mixed (Fig. 2G). Thus, the interlinking of signaling and cell sorting is required for cell fate divergence and spatial ordering.

Synthetic assembly is robust, reversible, and self-repairing

To see how reproducibly the synthetic cell-cell signaling program could drive three-layer formation, we followed 28 independent replicate cocultures starting with 200 A-type cells and 40 B-type cells (Fig. 3A). In most wells (57%), cells formed a single three-layer spheroid. In other wells, we observed "twin" multicore three-layer spheroids (21%) or multiple (separate) three-layer spheroids in the same well (11%).

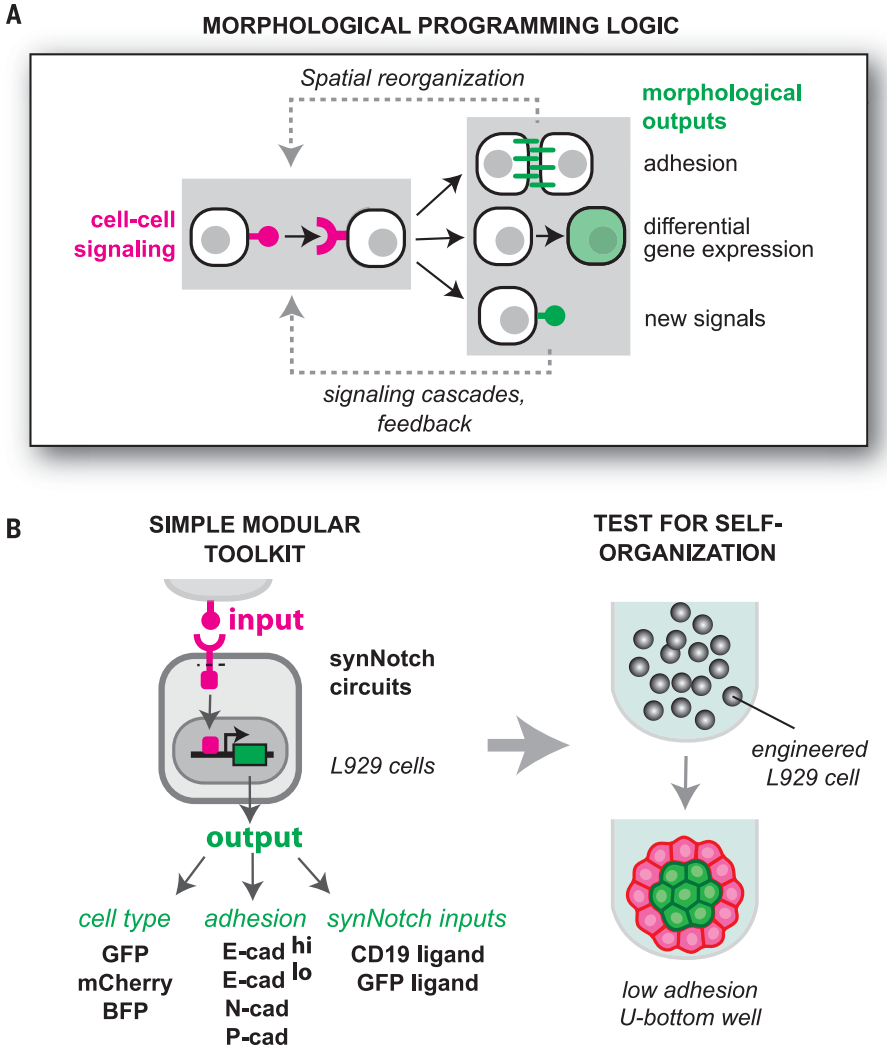

Fig. 1. Engineering cell-cell communication networks to program synthetic morphogenesis. (**A**) Design logic underlying our synthetic morphogenesis circuits. Engineered cell-cell signaling is used to drive changes in cell adhesion, differentiation, and production of new cell-cell signals. These outputs can subsequently be propagated to generate new cell-cell signaling relationships. (**B**) Molecular components used for assembly of simple morphological circuits. We used two synNotch ligand-receptor pairs (surface ligands CD19 and GFP) for cell signaling, three fluorescent proteins as markers of "differentiation," and several cadherin molecules (expressed at different levels) as morphological outputs. Engineered circuits are transduced into L929 fibroblast cells, placed in defined numbers in low-adhesion U-bottom wells, and screened by microscopy for spatial self-organization.

Thus, the overall three-layer architecture of green, red, and blue cells was robustly generated in ~90% of the cultures. A 3D reconstruction image of three-layer structure is shown in Fig. 3B and movie S1. Three-layer formation was robust to variation in the initial number or ratio of starting cells (fig. S2C). Only when we used a low number of starting A-type cells did we begin to see formation of two-layer structures (green and red only), because all the A-type cells were converted to $Ecad^{lo}$ cells (i.e., the number of A cells was limiting).

In many cases, natural self-organized tissues have an ability to regenerate after injury (*17*). To test how this three-layer structure would respond to injury, we cut the structure into two fragments with a microfluidic guillotine system (*18*) (movie S2). Immediately after cleavage, the GFP-positive core cells were exposed to the surface, but within 24 hours, the green core cells were re-enveloped by the red layer, regenerating the spherical three-layer structure (Fig. 3C). To further test the reversibility of the self-assembled three-layer structure, we added the synNotch inhibitor DAPT to preformed structures. The layered structure and distinct cell types were totally disrupted within 3 days of treatment; hence, this dynamically maintained structure can be disassembled by turning off cell-cell signaling (Fig. 3D).

A single-genotype circuit that induces cell fate bifurcation and spatial ordering into a two-layer structure

We also wanted to explore whether we could program self-organizing structures that could start from a single cell type. Alternative bistable

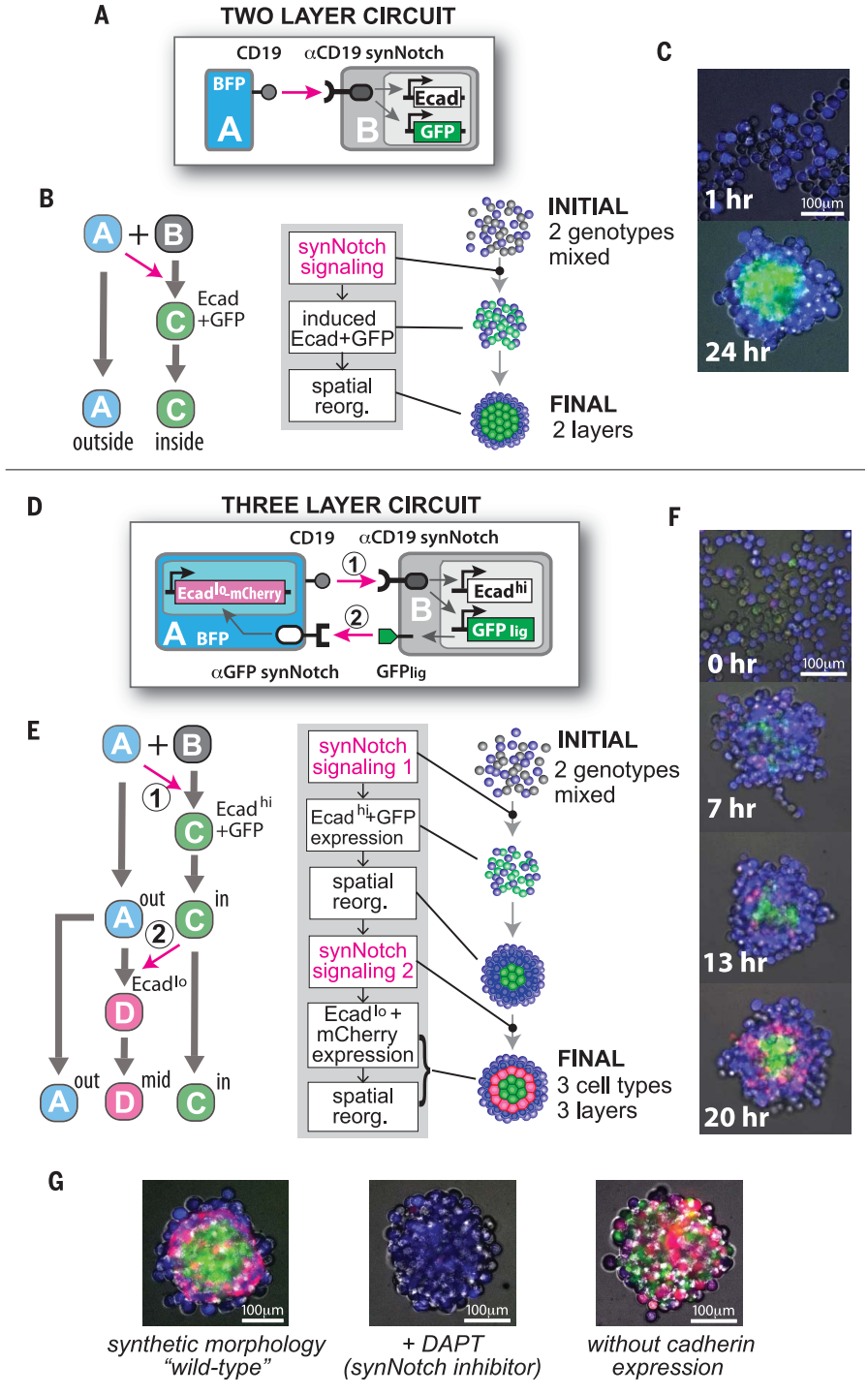

Fig. 2. Engineering self-organizing multilayered spheroids. (**A** to **C**) Two-layer circuit. (A) An A-type sender cell expressing CD19 ligand induces a B-type receiver cell to express E-cadherin and GFP. (B) SynNotch cell-cell signals drive receiver cells to express E-cadherin (Ecad), which leads to their segregation into a central layer. The system starts with two disordered cell genotypes but organizes to form a structure with two distinct spatial compartments. (C) Images of the spheroid at 1 and 24 hours. See fig. S1 for other data. (**D** to **G**) Three-layer circuit. (D) An A-type cell can send signals to a B-type cell using CD19 ligand, which induces expression of E-cadherin (high expression) and GFP_{lig} (surface-expressed GFP). The induced B-type cell can then send reciprocal signals to the A-type cell; GFP_{lig} serves as ligand to stimulate anti-GFP synNotch receptor expressed in the A-type cell. This reciprocal interaction is programmed to drive a low level of E-cadherin and mCherry. (E) Cell fate diagram showing how this program drives a two-step differentiation process in which the A→B synNotch signal first drives conversion of B-type cells to C-type cells that self-adhere and sort to the center of the structure. The sorted C-type cells then present the C→A synNotch signal (driven by GFP_{lig}) to convert spatially adjacent A-type cells into the middle-layer D-type cell (mCherry and low-level E-cadherin expression). A-type cells bifurcate into two phenotypes, depending on their spatial proximity to the C-type cells in the core of the structure. Here, the system starts with two disordered cell genotypes but self-organizes into three distinct cell phenotypes organized into three spatially distinct compartments. (F) Images from the development of the three-layer system from 0 to 20 hours. See fig. S2 and movie S1 for other data and time-lapse videos. (G) Formation of the three-layer structure is disrupted if synNotch signaling is inhibited (using DAPT, a γ-secretase inhibitor) or if cadherins are not driven as outputs. See fig. S3 for more information.

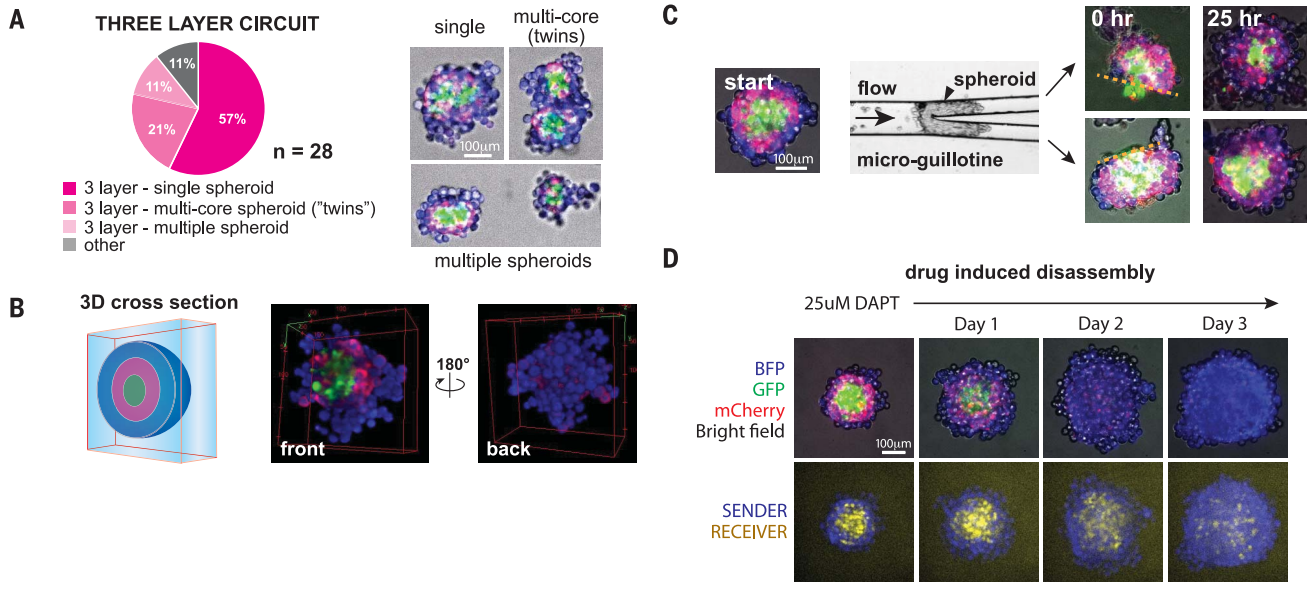

Fig. 3. Three-layer self-organized structure is robust, reversible, and self-repairing. (**A**) Distribution of structures generated in 28 independent wells (starting with 200 A-type cells and 40 B-type cells). About 90% of the wells showed formation of three-layer structures; the majority of these showed one spheroid per well, with the remainder showing either twinned spheroids or multiple independent three-layer spheroids. Example images of these structural subtypes are shown at the right. (**B**) Three-dimensional confocal reconstruction of a three-layer structure cross section, shown from two views. See movie S1 for full rotational view of the 3D structure. (**C**) Self-repair of a cleaved three-layer structure. The preformed spheroid was cleaved using a microfluidic guillotine, and the two resulting fragments were observed for 25 hours. The frames at 0 hours show the two fragments, with a dotted line indicating the cleavage plane that exposes the internal core of the spheroid. Images at 25 hours show self-repair of the spherical three-layer structure. (**D**) The structure is reversible if treated with the synNotch inhibitor DAPT. Within 3 days, the differentiation and spatial organization of cells disappeared. Original A- and B-type cells became randomly organized.

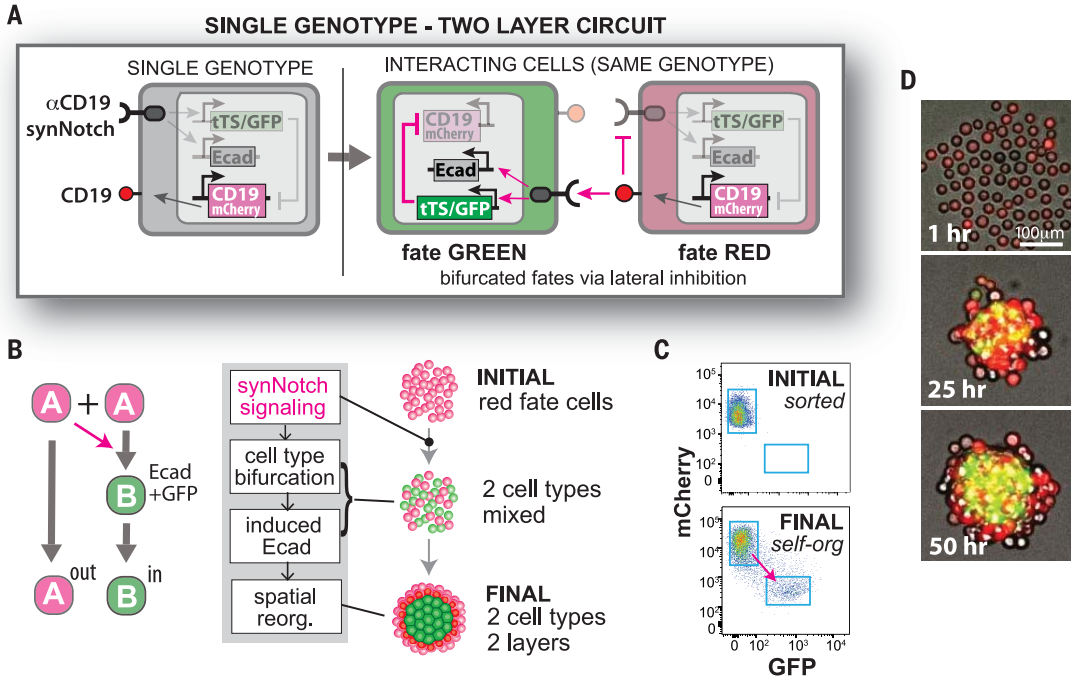

Fig. 4. Single-genotype circuit that induces fate bifurcation and spatial ordering into a two-layer structure. (**A**) Design of single-genotype circuit with lateral inhibition between sender (CD19^{+}) and receiver (antiCD19-synNotch–activated) states. The cell encodes both CD19 and anti-CD19 synNotch, but activated synNotch receptor drives expression of tet repressor (tTS), which inhibits CD19 expression. Thus, neighboring cells will drive each other into opposite states indicated by red and green fluorescent markers (fate RED and GREEN). (**B**) E-cadherin expression driven from the synNotch-activated promoter. An initially homogeneous population of red cells undergoes bifurcation into RED fate and Ecad-positive GREEN fate by lateral inhibition, and GREEN-fate cells are finally sorted inside to form an inner core. The system starts with a single-genotype population but is expected to organize into a two-layer structure. (**C**) Purification of a homogeneous population by sorting for mCherry^{high}/GFP^{low} cells. When allowed to communicate through lateral inhibition, the cells rebifurcate into two distinct fluorescently labeled populations (bottom). See fig. S4 and supplementary materials for more information on how the lateral inhibition circuit was constructed and executed. (**D**) Development of the single-genotype two-layer structure. Time frames are shown at 1, 25, and 50 hours, showing initial cell fate bifurcation followed by formation of a stable two-layer structure. See fig. S5 for more information and movie S3 for time-lapse video.

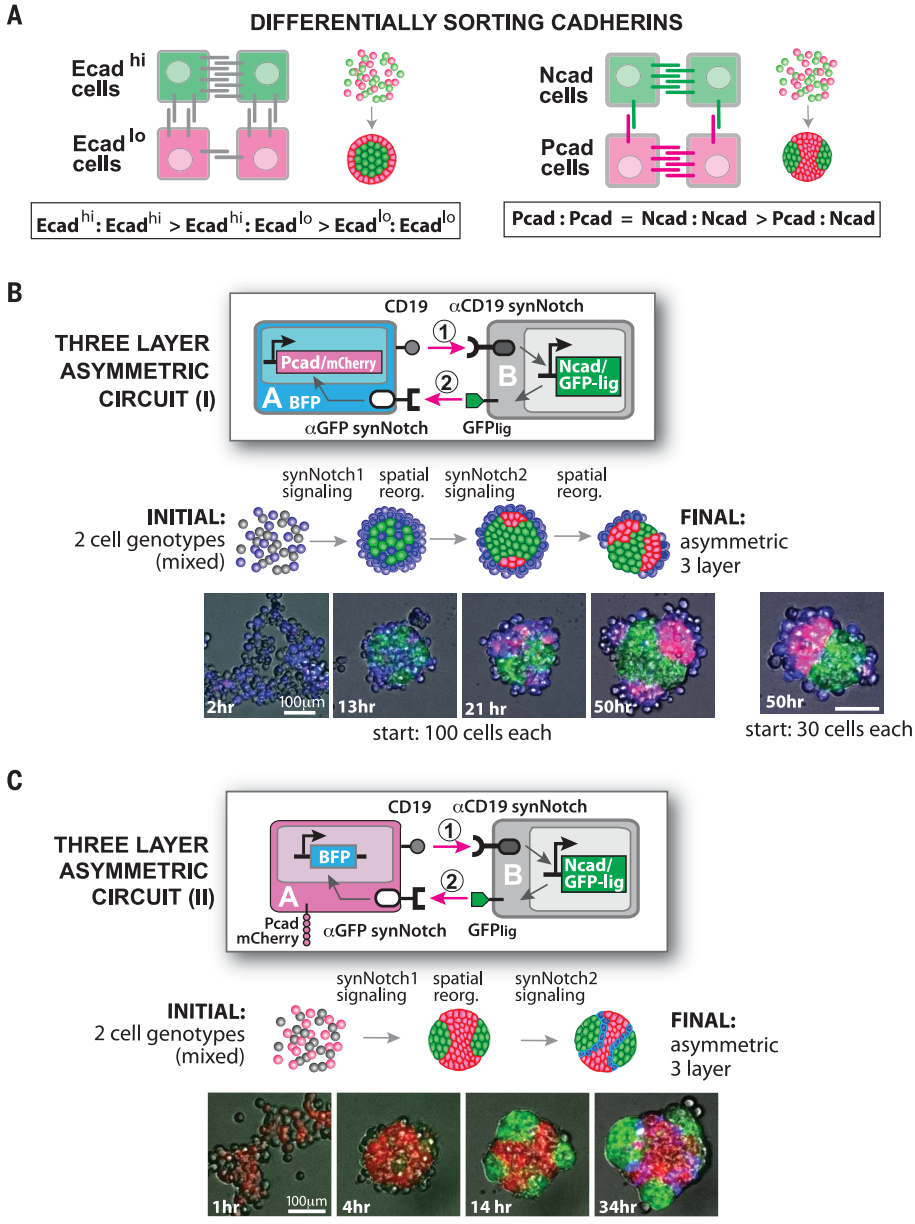

Fig. 5. Programming spherically asymmetric structures by inducing differentially sorting adhesion molecules. (**A**) Logic of deploying alternative adhesion outputs to generate different spatial structures. In the spherically symmetric structures of Figs. 2 to 4, we used high and low levels of Ecad expression to define different populations of cells. High- and low-Ecad populations lead to sorting into concentric shells, because $Ecad^{lo}$ cells still prefer to bind $Ecad^{hi}$ cells. In contrast, two cell populations that express either Ncad or Pcad will sort into distinct compartments (nonconcentric) because each of these cadherins prefers homotypic self-association to heterotypic cross-association. (**B**) Three-layer asymmetric circuit I, with the same architecture as that shown in Fig. 2, except that B-type cells are induced to express Ncad and A-type cells are induced to express Pcad. In phase II of the development (reciprocal B→A signaling), the A-type cells become red and self-sort to form one to three external poles (with unactivated A-type cells associated at their periphery). The starting population included 100 cells of each type. When we started with only 30 cells of each type (right image), we reproducibly generated single-pole structures. See fig. S7 and movie S4 for more information, time-lapse videos, and 3D structure. (**C**) Three-layer asymmetric circuit II. An A-type cell constitutively expresses Pcad and mCherry as well as CD19 ligand. B-type cells recognize CD19 with anti-CD19 synNotch receptor, which drives expression of Ncad and GFP_{lig}. In reciprocal signaling, GFP_{lig} drives induction of a BFP marker in A-type cells. Here, the red A-type cells first form a central core and the induced green B-type cells form polar protrusions. A third cell type (blue) forms at the boundary between the red core and the green protrusions. See fig. S8 and movie S5 for more information, time-lapse video, and 3D structure. Information on other structures using different cadherin pairs is shown in figs. S9 and S10 and movies S6 and S7.

cell fates can be generated from a single starting cell genotype through a mechanism known as lateral inhibition (*19*). For example, cross-repression between Notch receptor and its ligand in neighboring cells can result in a bistable, checkerboard fate pattern, where individual cells bifurcate into either $Notch^{active}$-$ligand^{low}$ or $Notch^{inactive}$-$ligand^{high}$ states (*20*, *21*). We built an analogous lateral inhibition circuit using synNotch cross-repression in L929 cells (fig. S4B). Each cell encoded both CD19 (ligand) and the anti-CD19 synNotch receptor, but these are antagonistic to each other because the synNotch receptor induces expression of the Tet repressor (tTS), which can repress CD19 expression (controlled by a TetO promoter). Thus, if synNotch is stimulated by a neighboring cell with high CD19 expression, it will repress CD19 ligand expression, thereby forcing cells to choose between either a sender or receiver fate. CD19 and tTS expression were monitored by mCherry and GFP, respectively (expressed in linked transcriptional cassettes through a ribosomal skipping porcine teschovirus-1 2A sequence). We established multiple clones that bifurcated spontaneously into two populations of mCherry or GFP-positive cells (fig. S4B; see supplementary materials for details of how we established lateral inhibition lines). These cell lines consistently reestablished the two phenotypic states, even when starting with a pure sorted population of either the red or green state (Fig. 4C and fig. S4B).

To produce a spatially ordered structure from a single cell type, we then functionally combined two different organizational circuit modules: this bifurcating cell fate circuit and the self-organized E-cadherin–driven two-layer circuit (Fig. 2A). To construct such a composite circuit, we expressed E-cadherin from the synNotch-driven promoter (in addition to inducing expression of the tet repressor) (Fig. 4A and fig. S5A). The objective was to start with a single cell type and observe self-driven fate bifurcation followed by self-driven sorting into two layers.

To track how the system developed from a single cellular phenotype, we sorted red-fate cells ($CD19_{high}$), placed 100 cells in each well, and followed the development of the spheroid by time-lapse microscopy. These cells developed into a spheroid in which the cells first underwent bifurcation into a red-green checkerboard pattern and then, over the course of hours, formed a two-layer structure with green cells inside and red cells outside (fig. S5, B and C). These two-layer structures were stable for 100 hours. Addition of the Notch signaling inhibitor DAPT prevented fate bifurcation (fig. S5C). But after removal of the drug and re-sorting, the cells remained bipotent; they could still bifurcate and

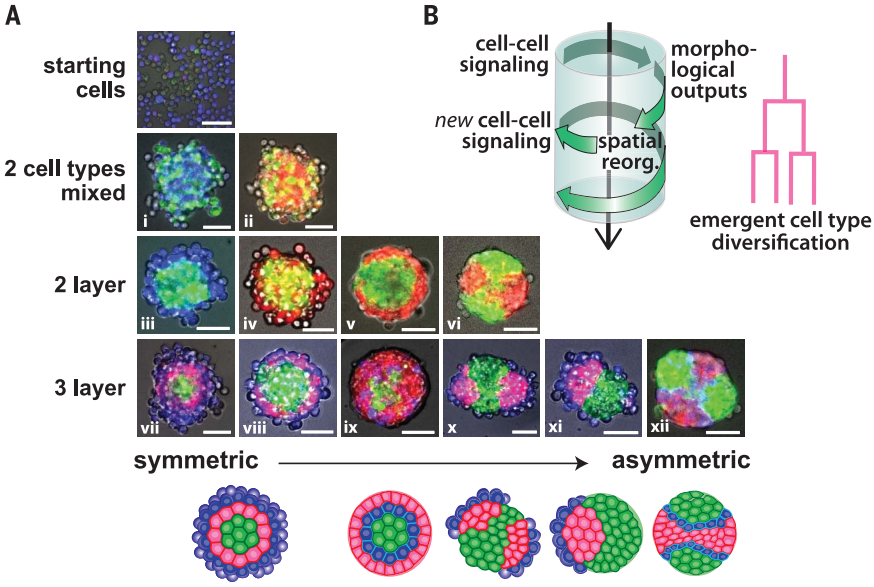

Fig. 6. Gallery of different self-organizing multicellular structures that can be programmed using the simple synNotch→adhesion toolkit. (**A**) Gallery of spatially organized behaviors generated in this work, organized by resulting number of cell types and spatially distinct compartments as well as by increasing asymmetry. See table S1 for details of the construction of these 12 structures. Diagrams of several of the different three-layer structures are shown schematically below. (**B**) These synthetic developmental systems share the common principles in which cascades of cell-cell signaling, linked by morphological responses, lead to increasing diversification of cell types. As signaling drives morphological changes and reorganization, new cell-cell interactions arise, resulting in increasingly distinct positional information encountered by each cell in the structure.

reform the two-layer structure (Fig. 4D, fig. S5C, and movie S3). Thus, we can engineer synthetic programs in which a single cell genotype bifurcates and spatially self-organizes into multiple layers.

Programming spherically asymmetric structures by inducing differentially sorting cell adhesion molecules

Another key feature of natural morphogenesis is symmetry breaking, used repeatedly during development to generate body axes and elaborate an initially uniform ball of cells (*22*, *23*). The structures described above are all spherically symmetric, but we could program asymmetric structure formation with the same signaling cascade circuit by simply changing the adhesion molecules that were expressed.

To build the spherically symmetric three-layer structure described above (Fig. 2D), we programmed different subsets of cells to express different amounts of the same adhesion molecule (E-cadherin), which generates spherically symmetric concentric layers (because $Ecad^{lo}$ cells still prefer to interact with $Ecad^{hi}$ cells; see relative interaction energies in Fig. 5A). However, if cells express different cadherins that have high homotypic affinity but low heterotypic affinity, they phase-separate into two spatially distinct populations (Fig. 5A). N-cadherin (Ncad) and P-cadherin (Pcad) have high homotypic affinity (Ncad-Ncad and Pcad-Pcad) but low heterotypic affinity (Ncad-Pcad) (*24*), so we used the combination of Ncad and Pcad expression to try to drive asymmetric sorting and structure formation (fig. S6).

We introduced Ncad and Pcad as morphological outputs in the basic three-layer circuit. First, CD19 synNotch signaling from cell A induced expression of Ncad and GFP_{lig} in cell B; second, the induced GFP_{lig} on cell B reciprocally activated anti-GFP synNotch in the adjacent subpopulation of A cells, driving Pcad expression (Fig. 5B, fig. S7, and movie S4). When we cultured 100 cells each of type A and B together, we observed a stereotypical developmental sequence: By 13 hours, B-type cells expressed both Ncad and GFP_{lig}, and by 21 hours, A-type cells adjacent to B-type cells began to express Pcad and mCherry. Because of the resulting self-segregation of the Ncad- and Pcad-expressing cells, the ensemble self-organized into a nonspherically symmetric three-layer structure (green, red, blue) with one to three distinct poles of mCherry (Pcad) cells. A-type cells (blue) not activated through their anti-GFP synNotch receptors were associated with the outer surface of these poles.

When we initiated cultures with a smaller number of starting cells (30 cells each of type A and B), the ensemble reproducibly formed a single-pole asymmetric structure (a single cluster of red cells instead of multiple clusters), consistent with many examples of polarized organization in which a smaller starting size minimizes the chance of initiation of multiple independent poles (Fig. 5B, fig. S7, and movie S4) (*25*). Thus, we could reliably program systems that would form three-layer asymmetric or polarized structures.

We designed other circuits that induced alternative types of asymmetric structures with the same Ncad-Pcad output combination but were regulated in different sequential programs. In the circuit shown in Fig. 5C, cell A was similar to the above example (it expressed CD19 ligand and anti-GFP synNotch receptor driving expression of BFP), except that it also constitutively expressed Pcad [connected with mCherry via an internal ribosome entry site (IRES) sequence]. Cell B was the same as in Fig. 5B (it expressed anti-CD19 synNotch receptor that induced Ncad and GFP_{lig} expression). When cultured together, the Pcad-expressing A cells (red) immediately formed an adherent aggregate (4 hours); then, after 14 hours, Ncad and GFP_{lig} were expressed in B-type cells, leading to the formation of polarized B-type protrusions (green) segregated from the A-type cells (red). Finally, at 34 hours, A-type cells at the interface with B-type cells were activated by GFP-synNotch signaling to turn on BFP, resulting in a thin boundary layer of blue cells between the polarized red and green regions (time-lapse and 3D reconstruction image shown in fig. S8 and movie S5). Additional types of combinatorial circuits using different cadherin pairs are shown in figs. S9 and S10 and in movies S6 and S7.

These results confirmed that we can build various self-organizing structures that break spherical symmetry by inducing distinct self-segregating adhesion molecules in different subpopulations of cells. Initial conditions with small cell numbers can reproducibly yield structures with a single polar axis. Moreover, we can generate many different three-layer morphological structures by altering the combinations of adhesion molecules used and by altering at what stage in the circuit they are expressed (Figs. 5 and 6).

Minimal intercellular communication programs can drive synthetic self-organizing cellular structures

Figure 6A and table S1 summarize the various self-organizing synthetic structures we programed with our minimal logic of controlling cell adhesion (cadherin expression) through cell-cell communication (synNotch signaling). The diversity and complexity of these structures, and the robustness with which they are formed, illustrate the ordering power of even these highly simplified cell-cell signaling programs. In all of these systems, we observed a cyclic sequence of events in which initial cell signaling interactions induced morphological rearrangements, which in turn generated new cell-cell interactions and new morphological refinements (Fig. 6B). Complex structures emerge because these cell-cell signaling cascades drive increasing cell type diversification.

These diverse emergent structures can form even in the absence of many of the molecular components normally used in natural developmental systems. For example, these circuits do not incorporate diffusible morphogens for cell-cell communication, irreversible cell fate commitment, or direct regulation of cell proliferation, death, or motility (*8*, *26*–*29*). It is likely that the

synthetic platforms used here could be extended to include many of these additional elements to generate even more sophisticated engineered self-organizing multicellular structures (*30*–*35*).

The observation that even minimal circuits that link cell-cell signaling to adhesion can lead to the formation of defined self-organizing structures may help to explain the general principles by which multicellular organisms could have evolved. Choanoflagellates, the closest single-cell relatives of metazoans, have both primitive cadherin and notch genes (*36*). The cadherin genes are thought to have originally functioned to trap prey bacteria in the environment and may have later been co-opted for cell-cell adhesion (*37*, *38*). In some choanoflagellate species, environmental signals from prey bacteria can induce the formation of multicellular assemblies (*39*, *40*). It seems plausible that cell-to-bacteria adhesion transitioned to cell-cell adhesion, and that bacteria-to-cell signaling transitioned to cell-cell signaling. During the course of evolution, these systems may have begun to regulate one another, providing a starting point for circuits capable of driving formation of complex multicellular structures.

More generally, these findings suggest that it may be possible to program the formation of synthetic tissues, organs, and other non-native types of dynamic, multicellular materials. We may be able to apply tools like synNotch, perhaps enhanced by an even larger toolkit of modular developmental signals, to construct customized self-assembling tissue-like biomaterials of diverse types. These tools and approaches also provide powerful tools to systematically probe and better understand the principles governing self-organization and development.

REFERENCES AND NOTES

1. J. Davies, *Development* **144**, 1146–1158 (2017).
2. M. Elowitz, W. A. Lim, *Nature* **468**, 889–890 (2010).
3. B. P. Teague, P. Guye, R. Weiss, *Cold Spring Harb. Perspect. Biol.* **8**, a023929 (2016).
4. A. Kicheva, N. C. Rivron, *Development* **144**, 733–736 (2017).
5. S. Basu, Y. Gerchman, C. H. Collins, F. H. Arnold, R. Weiss, *Nature* **434**, 1130–1134 (2005).
6. S. S. Jang, K. T. Oishi, R. G. Egbert, E. Klavins, *ACS Synth. Biol.* **1**, 365–374 (2012).
7. M. Rubenstein, A. Cornejo, R. Nagpal, *Science* **345**, 795–799 (2014).
8. L. Wolpert, *J. Theor. Biol.* **25**, 1–47 (1969).
9. D. Gilmour, M. Rembold, M. Leptin, *Nature* **541**, 311–320 (2017).
10. L. Morsut *et al*., *Cell* **164**, 780–791 (2016).
11. A. Nose, A. Nagafuchi, M. Takeichi, *Cell* **54**, 993–1001 (1988).
12. D. Duguay, R. A. Foty, M. S. Steinberg, *Dev. Biol.* **253**, 309–323 (2003).
13. R. A. Foty, M. S. Steinberg, *Dev. Biol.* **278**, 255–263 (2005).
14. M. Vinci *et al*., *BMC Biol.* **10**, 29 (2012).
15. C. Chazaud, Y. Yamanaka, *Development* **143**, 1063–1074 (2016).
16. S. E. Harrison, B. Sozen, N. Christodoulou, C. Kyprianou, M. Zernicka-Goetz, *Science* **356**, eaal1810 (2017).
17. A. Sánchez Alvarado, P. A. Tsonis, *Nat. Rev. Genet.* **7**, 873–884 (2006).
18. L. R. Blauch *et al*., *Proc. Natl. Acad. Sci. U.S.A.* **114**, 7283–7288 (2017).
19. J. R. Collier, N. A. M. Monk, P. K. Maini, J. H. Lewis, *J. Theor. Biol.* **183**, 429–446 (1996).
20. S. J. Bray, *Nat. Rev. Mol. Cell Biol.* **7**, 678–689 (2006).
21. M. Matsuda, M. Koga, K. Woltjen, E. Nishida, M. Ebisuya, *Nat. Commun.* **6**, 6195 (2015).
22. S. Wennekamp, S. Mesecke, F. Nédélec, T. Hiiragi, *Nat. Rev. Mol. Cell Biol.* **14**, 452–459 (2013).
23. S. C. van den Brink *et al*., *Development* **141**, 4231–4242 (2014).
24. J. Vendome *et al*., *Proc. Natl. Acad. Sci. U.S.A.* **111**, E4175–E4184 (2014).
25. E. Cachat *et al*., *Sci. Rep.* **6**, 20664 (2016).
26. A. M. Turing, *Philos. Trans. R. Soc. London Ser. B* **237**, 37–72 (1952).
27. M. D. Jacobson, M. Weil, M. C. Raff, *Cell* **88**, 347–354 (1997).
28. E. Scarpa, R. Mayor, *J. Cell Biol.* **212**, 143–155 (2016).
29. E. Li, *Nat. Rev. Genet.* **3**, 662–673 (2002).
30. J. A. Davies, *J. Anat.* **212**, 707–719 (2008).
31. S. A. Newman, R. Bhat, *Int. J. Dev. Biol.* **53**, 693–705 (2009).
32. Y. E. Antebi, N. Nandagopal, M. B. Elowitz, *Curr. Opin. Syst. Biol.* **1**, 16–24 (2017).
33. J. B. A. Green, J. Sharpe, *Development* **142**, 1203–1211 (2015).
34. Y. Hart *et al*., *Cell* **158**, 1022–1032 (2014).
35. Y. Okabe, R. Medzhitov, *Nat. Immunol.* **17**, 9–17 (2016).
36. N. King *et al*., *Nature* **451**, 783–788 (2008).
37. M. Abedin, N. King, *Science* **319**, 946–948 (2008).
38. S. A. Nichols, B. W. Roberts, D. J. Richter, S. R. Fairclough, N. King, *Proc. Natl. Acad. Sci. U.S.A.* **109**, 13046–13051 (2012).
39. R. A. Alegado *et al*., *eLife* **1**, e00013 (2012).
40. A. Woznica *et al*., *Proc. Natl. Acad. Sci. U.S.A.* **113**, 7894–7899 (2016).

ACKNOWLEDGMENTS

We thank B. Honig and L. Shapiro for discussions regarding cadherin sorting and for providing cadherin plasmids, O. Klein for comments, members of the Lim Lab and the Morsut lab for discussion and assistance, and K. Roybal, M. Thomson, Z. Gartner, W. Marshall, J. Fung, and members of the UCSF Center for Systems and Synthetic Biology and the NSF Center for Cellular Construction. **Funding:** Supported by Japan Society for the Promotion of Science (JSPS) Overseas Research Fellowships (S.T.); a Human Frontiers of Science Program (HFSP) (S.T. and L.M.); a European Molecular Biology Organization (EMBO) Postdoctoral Fellowship (L.M.); NIH grants K99 1K99EB021030 (L.M.), 5P50GM081879 (W.A.L.), and T32GM008412 (L.R.B.); NSF DBI-1548297 Center for Cellular Construction (W.A.L. and S.K.Y.T.); the DARPA Engineered Living Materials program; and the Howard Hughes Medical Institute (W.A.L.). **Author contributions:** S.T. developed and planned research, carried out the design, construction, and testing of self-organizing circuits, and wrote the manuscript; L.R.B. designed and built the microfluidic guillotine and executed experiments for testing regeneration; S.K.Y.T. designed and conceptualized the microfluidic guillotine; L.M. developed and planned research and wrote and edited the manuscript; and W.A.L. developed, planned, and oversaw research and wrote and edited the manuscript. **Competing interests:** The synNotch platform has been patented (U.S. Patent 9,670,281) by the Regents of the University of California and is licensed by Gilead Biosciences. W.A.L. has a financial interest in Gilead Biosciences. **Data and materials availability:** All constructs will be made available on Addgene, and all relevant data are included within the main paper or the supplementary materials.

SUPPLEMENTARY MATERIALS

www.sciencemag.org/content/361/6398/156/suppl/DC1
Materials and Methods
Figs. S1 to S10
Table S1
Movies S1 to S7
References (*41*, *42*)

17 January 2018; accepted 22 May 2018
Published online 31 May 2018
10.1126/science.aat0271

Programming self-organizing multicellular structures with synthetic cell-cell signaling

Satoshi Toda, Lucas R. Blauch, Sindy K. Y. Tang, Leonardo Morsut, and Wendell A. Lim

Science **361** (6398), . DOI: 10.1126/science.aat0271

Engineering multilayered cellular structures

The ability to program the manufacture of biological structures may yield new biomaterials or synthetic tissues and organs. Toda *et al.* engineered mammalian "sender" and "receiver" cells with synthetic cell surface ligands and receptors that controlled gene regulatory circuits based on Notch signaling. Programming the cells to express cell adhesion molecules and other regulatory molecules enabled spontaneous formation of multilayered structures, like those that form during embryonic development. The three-layered structures even showed regeneration after injury.

Science, this issue p. 156